UHECRs and Extensive air showers

Ioana C. Mariș

New York University Abu Dhabi

Messenger particles

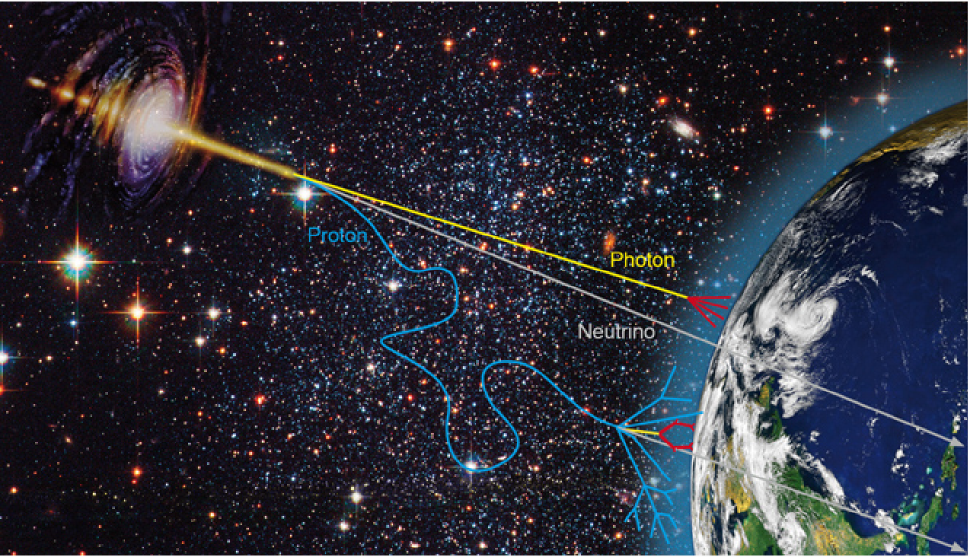

Some history

1896-1898 Becquerel, Marie y Pierre Curie

1909-1910 Theodor Wulf measurements on the Eiffel Tower

1907-1911 Domenico Pacini measurements in the sea

1912-1914 Baloon experiments: Gockel (4000 m), Hess (5200 m) y Kolhoester (9200 m) $\rightarrow$ radiation comes from above

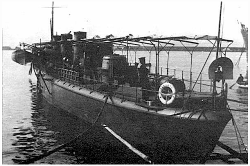

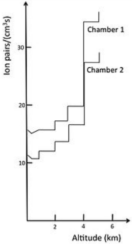

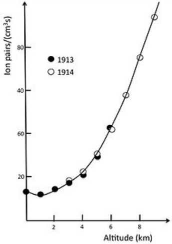

Air-showers

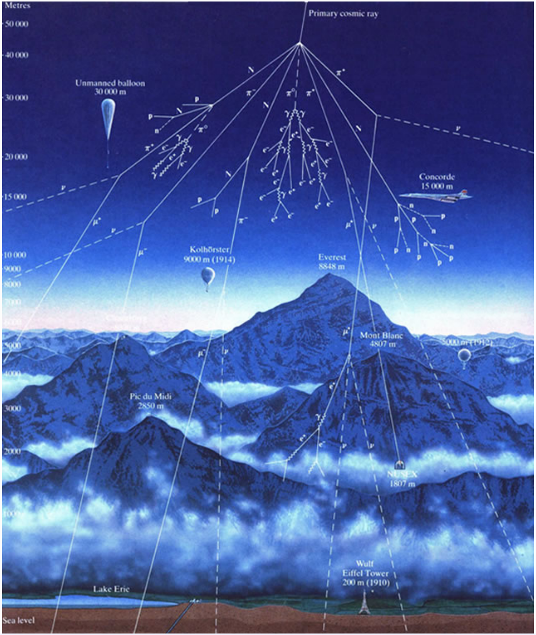

Pierre Auger

Bruno Rossi

1930 Pierre Auger y Bruno Rossi discover air-showers

1934 Anderson discoveres the positron, the first antiparticle

Particle accelarators

Large Hadron Collider

International Linear Collider

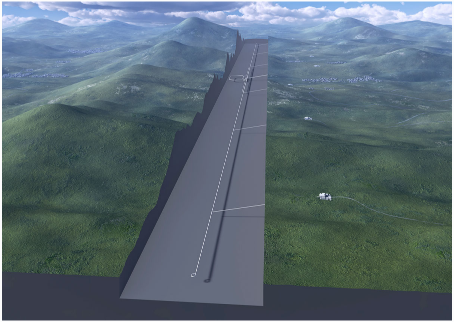

Energy: 14,000 GeV
Radius: 27 km

Energy: 500 GeV
Length: 30-50 km

Accelerators of cosmic rays

Huge Hadron Collider

Energy: 14,000,000 GeV
Radius: 58,000,000 km

Interplanetary Linear Collider

Energy: 10,000,000 GeV
Length: 1,400,000,000 km

How do we measure the air-showers?

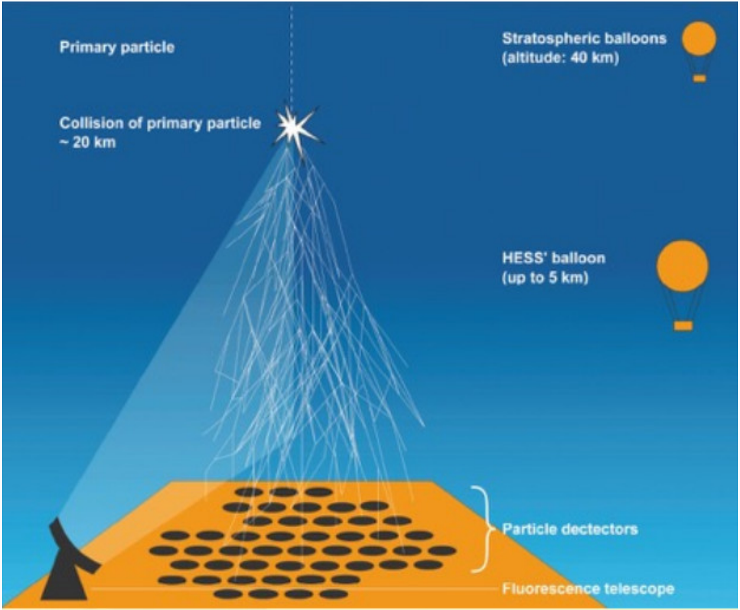

Telescope Array (Utah, USA)

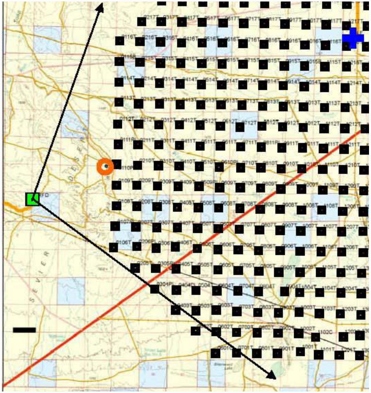

- Area: 750 km^2 ($\sim$ 0.25 Auger)
- 3 Fluorescence Detectors ($30^\circ \times 120^\circ$)
- 507 scintillators, 1.2 km
- Finished in 2008

Pierre Auger Observatory (Malargue Argentina)

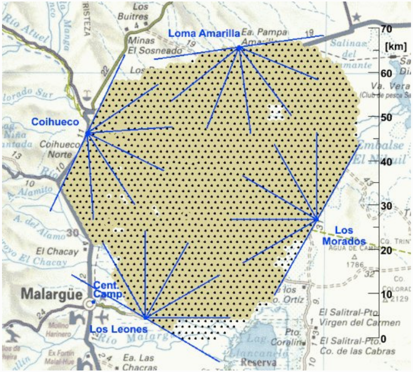

- Area: 3000 km^2
- 4 Fluorescence Detectors ($30^\circ \times 180^\circ$)
- 1665 Surface detectors
- Taking data since 2004, completed in 2008

Pierre Auger Observatory (Malargue Argentina)

- Area: 3000 km^2
- 4 Fluorescence Detectors ($30^\circ \times 180^\circ$)
- 1665 Surface detectors
- Taking data since 2004, completed in 2008

Enhancements of the Pierre Auger Observatory

Infill array

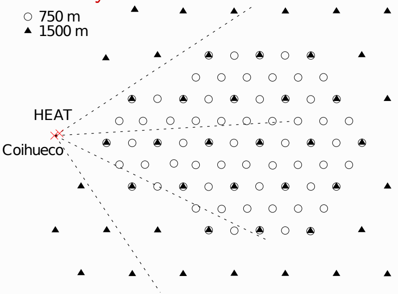

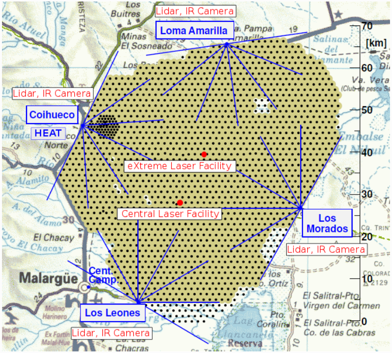

HEAT: High Elevation Auger Telescope

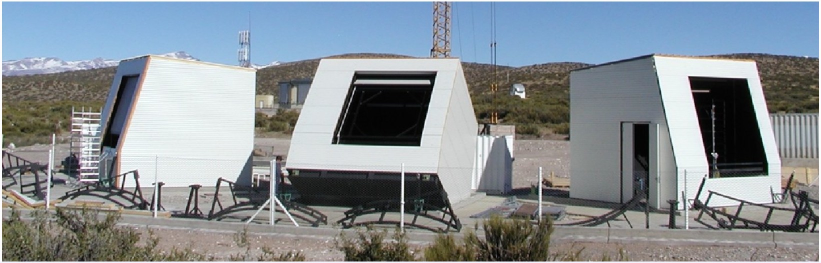

Air showers in Auger

We need to recontruct: direction, energy, mass of the primary particle

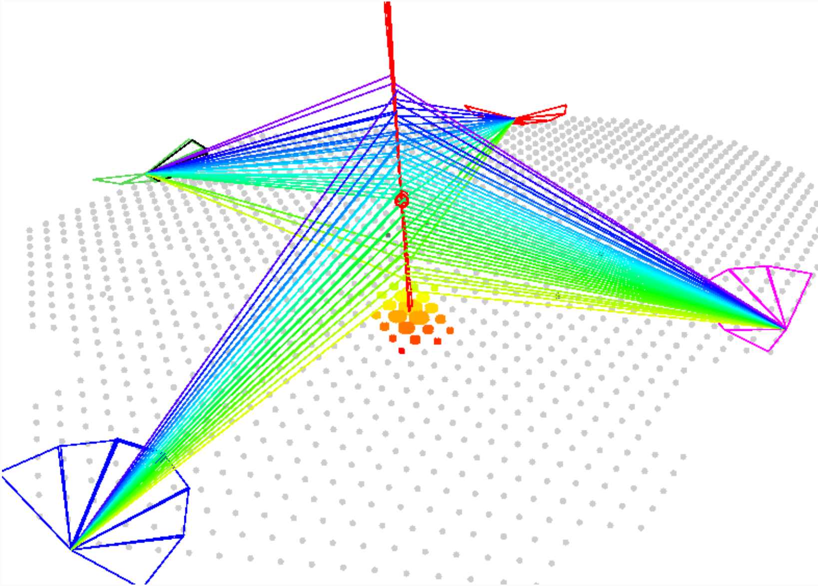

Hybrid Reconstruction

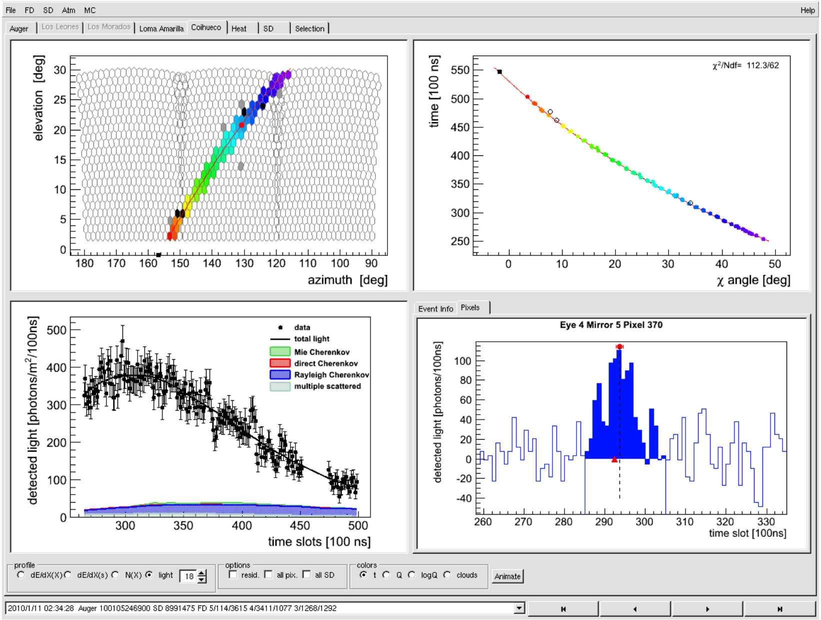

Hybrid Reconstruction

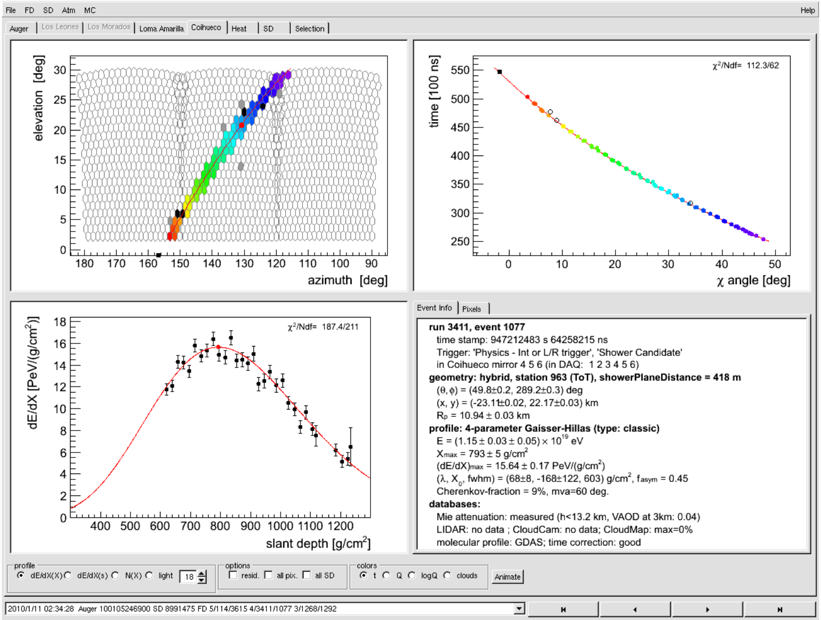

SD Reconstruction

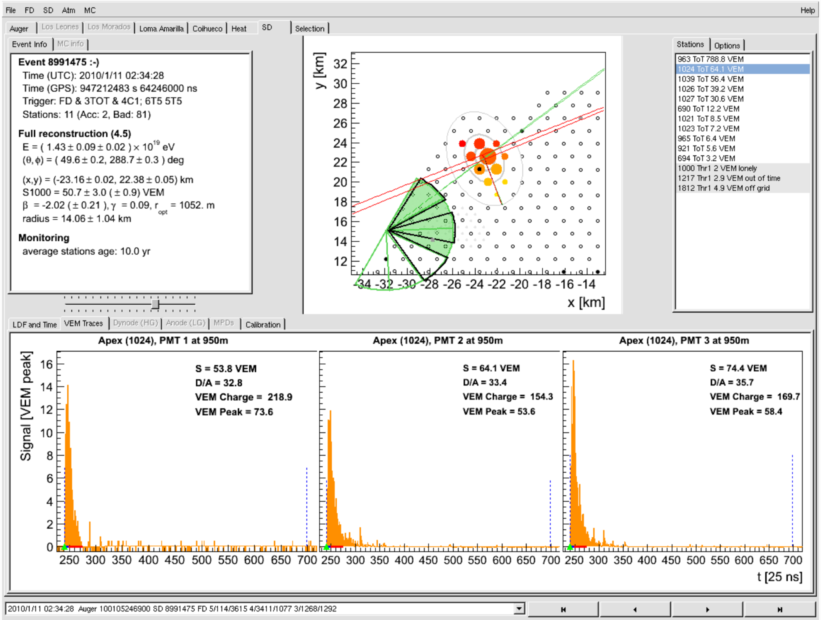

SD Reconstruction

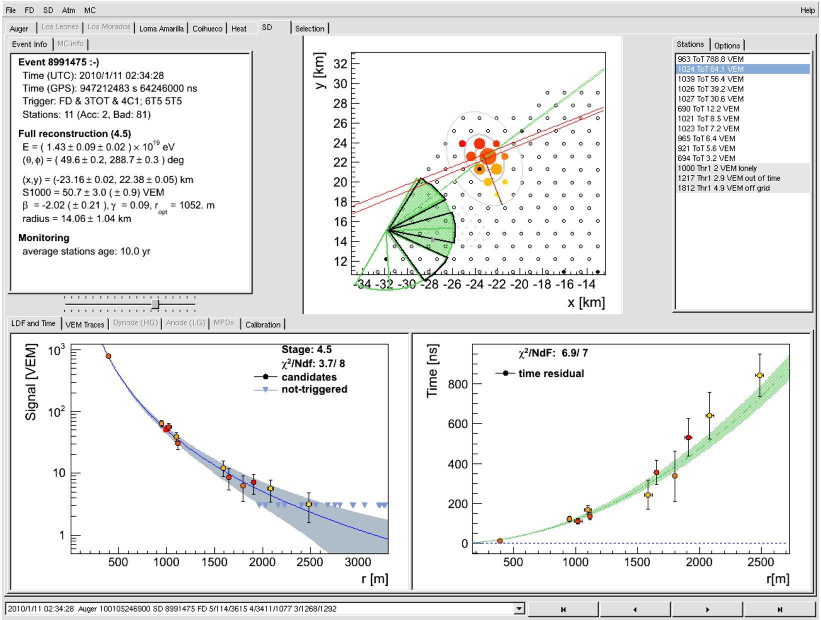

Air showers reconstruction

Event 201022604036, energy 72 ± 1 EeV, 54 degrees

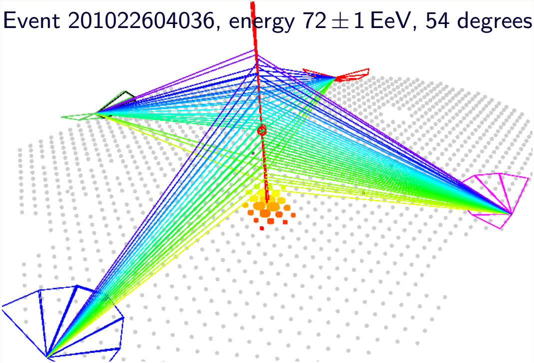

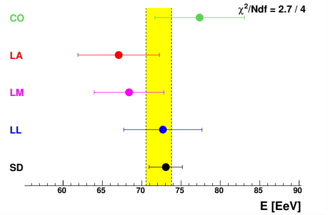

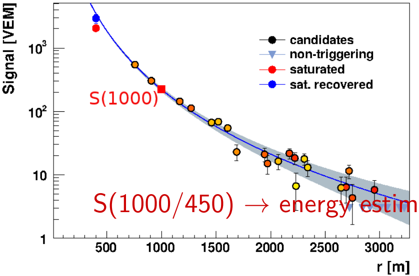

$S(1000/450) \rightarrow$ energy estimator

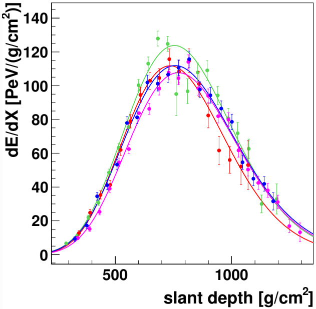

Energy: $\int$Gaisser-Hillas + invisible energy correction (10% @ 1 EeV, 8.5%@100 EeV)

Data sets at the Pierre Auger Observatory

SD vertical ($\theta < 60°$)

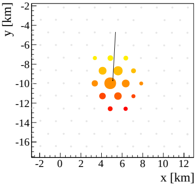

1500 m array

energy threshold:
$E = 3\,\mathrm{EeV}$

geometrical acceptance

SD infill ($\theta < 55°$)

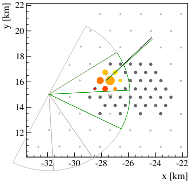

750 m array

energy threshold:
$E = 0.3\,\mathrm{EeV}$

geometrical acceptance

SD inclined ($62° < \theta < 80°$)

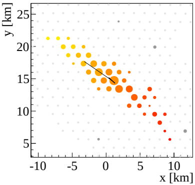

1500 m array

energy threshold:
$E = 4\,\mathrm{EeV}$

geometrical acceptance

Hybrid (FD + 1 SD station)

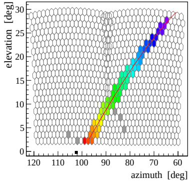

24 telescopes

energy threshold:
$E = 1\,\mathrm{EeV}$

acceptance from simulations

How is the measurement of the energy spectrum done?

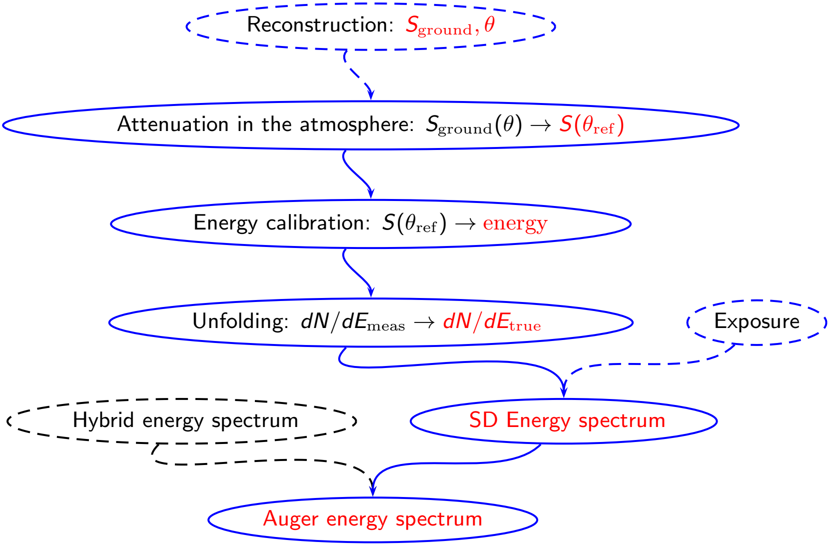

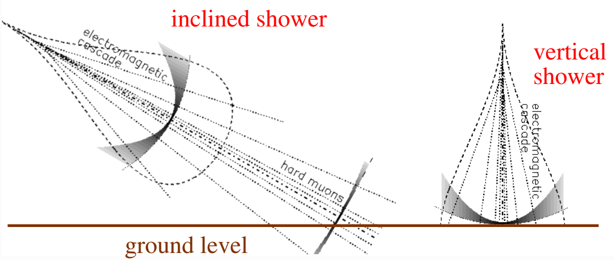

Method of Constant Intensity

integral cosmic ray flux is isotropic (local coordinates)

$$\frac{d\Phi}{d\Omega} \propto \frac{d\Phi}{d\cos\theta} \propto \frac{dI}{d\cos\theta A_{eff}} = const$$

intensity I (events above E_0)
projection on flat array geometry: $A_{\mathrm{eff}} = A\cos\theta$

$$\frac{dI}{d\cos^2\theta} = \mathrm{const}$$

S_{ground}:Attenuation in the atmosphere

empirical function
second degree polynomial in $\cos^2\theta$

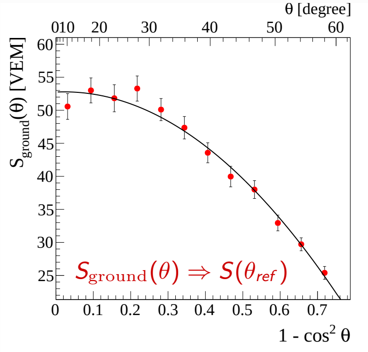

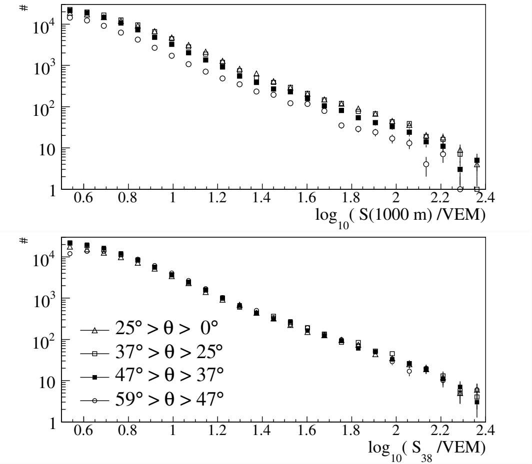

S_{ground}:Attenuation in the atmosphere

empirical function
second degree polynomial in $\cos^2\theta$

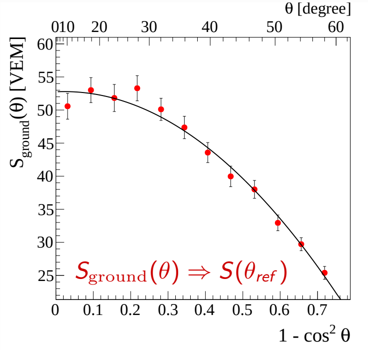

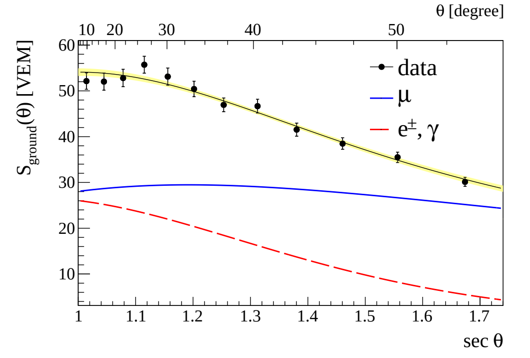

Physical interpretation

$$S_{\mathrm{ground}}(\theta) = N_{\mathrm{e.m.}} S_{\mathrm{e.m.}}(X(\theta)) g_{e.m.}(\theta) + N_{\mu} S_{\mu}(X(\theta)) g_{\mu}(\theta)$$

- modeling of the attenuation of air-showers and of the detector response

SD inclined events ($62^\circ < \theta < 80^\circ$)

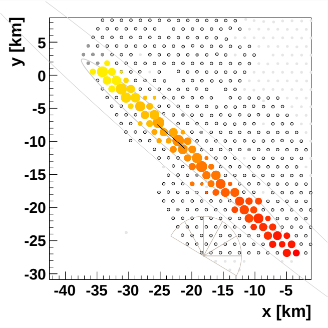

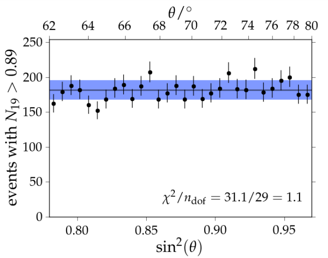

- only muonic component, muon density $n_\mu = f(x, y|\theta, \phi)$
- energy estimator, N_{19}, proportional to the number of muons and independent of the zenith angle $N_{19}(E, A) = N_\mu / N_\mu(10^{19}\,\mathrm{eV}, p, \theta)$
- reconstruction of events based on models for the muon density and on the full simulations (systematic uncertainty $N_{19} < 4\%$)

Energy calibration for the surface detector

- Energy calibration with events recorded by both FD and SD
- High quality events (+ fiducial field of view)

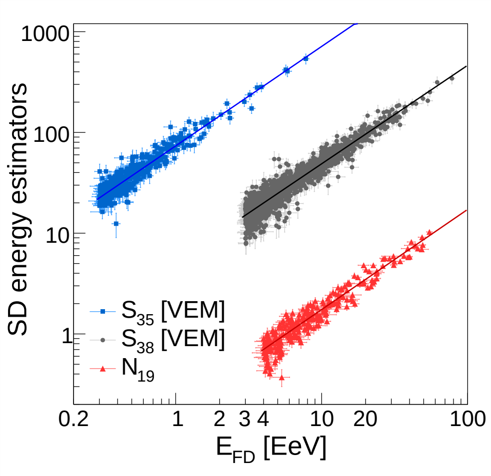

Calibration functions:
$E = A \cdot S^B$

- SD 1500 m:
  $A = (0.187 \pm 0.004)\,\mathrm{EeV}$
  $B = 1.023 \pm 0.007$
- SD inclined:
  $A = (5.71 \pm 0.1)\,\mathrm{EeV}$
  $B = 1.01 \pm 0.02$
- SD 750 m:
  $A = (12.87 \pm 0.6)\,\mathrm{PeV}$
  $B = 1.013 \pm 0.013$

SD energy resolution, 1500 m

obtained from the golden hybrid events

$E > 3\,\mathrm{EeV}$

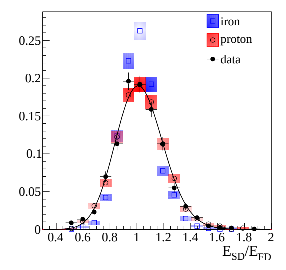

$\sigma_{SD}/E_{SD} = (16 \pm 1)\%$

$6\,\mathrm{EeV} < E < 10\,\mathrm{EeV}$

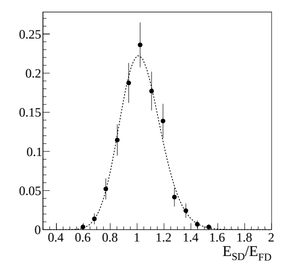

$\sigma_{SD}/E_{SD} = (13 \pm 1)\%$

$10\,\mathrm{EeV} < E$

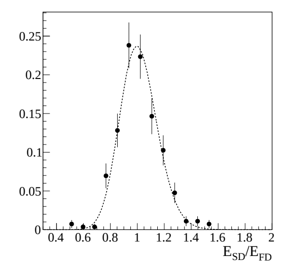

$\sigma_{SD}/E_{SD} = (11 \pm 1)\%$

Contributions:

- shower-to-shower fluctuations $\approx 10\%$
- reconstruction uncertainties 12% at 3 EeV and 6% above 10 EeV
- corrections for resolution effects with a forward folding procedure

Resolution correction through forward folding

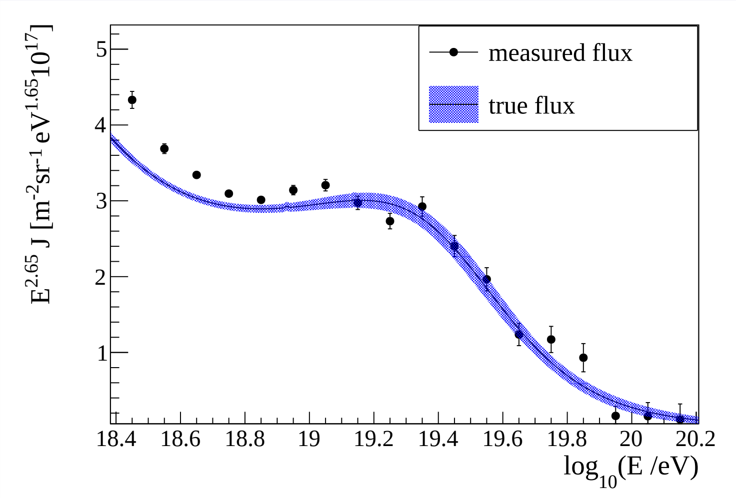

$$J_{\rm meas} = \mathbf{P}^{-1} \cdot \mathbf{R} \cdot \mathbf{P} J_{\rm true}$$

trigger efficiency **P**, response matrix **R** (air-showers and detector simulations)

Hybrid exposure

Detector fully efficient above 1 EeV

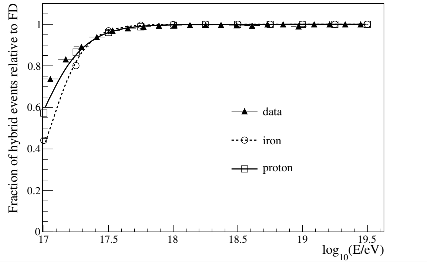

Relative difference to mixed composition

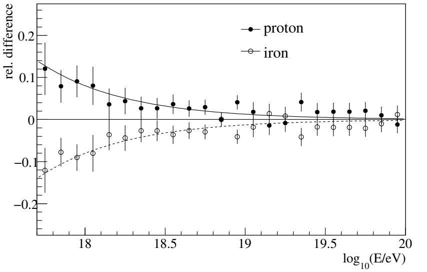

Cross-check with SD data

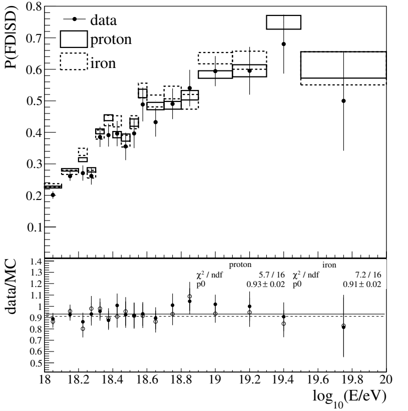

Energy systematics

Emission mechanism

Atmosphere

Calibration

Reconstruction

→ energy systematic uncertainty 14%

Absolute fluorescence yield	3.4%	
Fluores. spectrum and quenching param.	1.1%	
Sub total (Fluorescence Yield)	3.6%	14%
Aerosol optical depth	3% ÷ 6%	
Aerosol phase function	1%	
Wavelength dependence of aerosol scattering	0.5%	
Atmospheric density profile	1%	
Sub total (Atmosphere)	3.4% ÷ 6.2%	5.1% ÷ 7.6%
Absolute FD calibration	9%	
Nightly relative calibration	2%	
Optical efficiency	3.5%	
Sub total (FD calibration)	9.9%	9.5%
Folding with point spread function	5%	
Multiple scattering model	1%	
Simulation bias	2%	
Constraints in the Gaisser-Hillas fit	3.5% ÷ 1%	
Sub total (FD profile reconstruction)	6.5% ÷ 5.6%	10%
Invisible energy	3% ÷ 1.5%	4%
Statistical error of the SD calib. fit	0.7% ÷ 1.8%	
Stability of the energy scale	5%	
TOTAL	14%	22%

Measurements of the energy spectrum

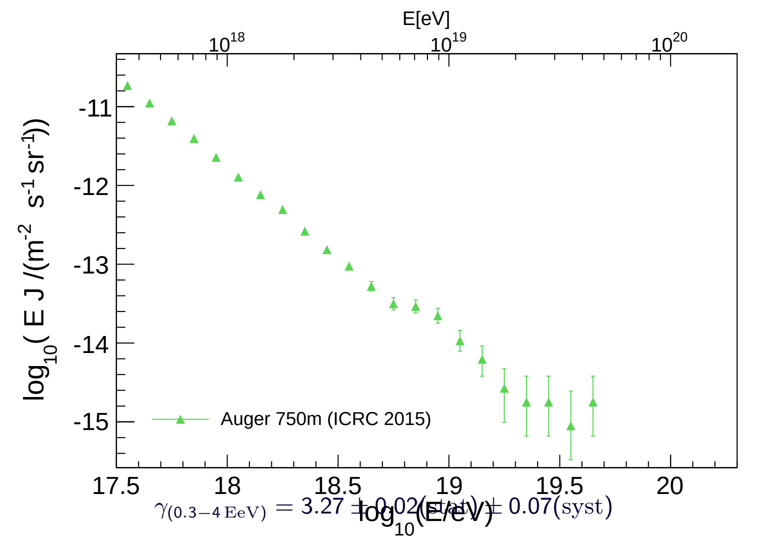

$$\gamma_{(0.3-4\,\mathrm{EeV})} = 3.27 \pm 0.02(\mathrm{stat}) \pm 0.07(\mathrm{syst})$$

Measurements of the energy spectrum

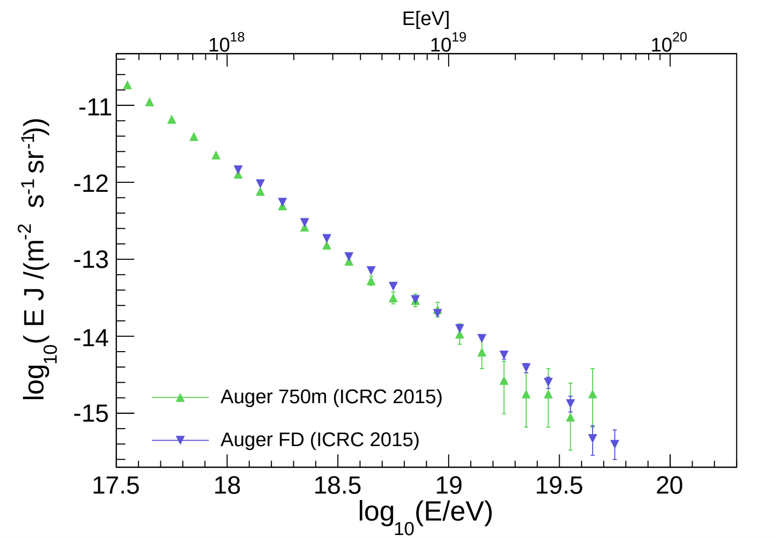

Measurements of the energy spectrum

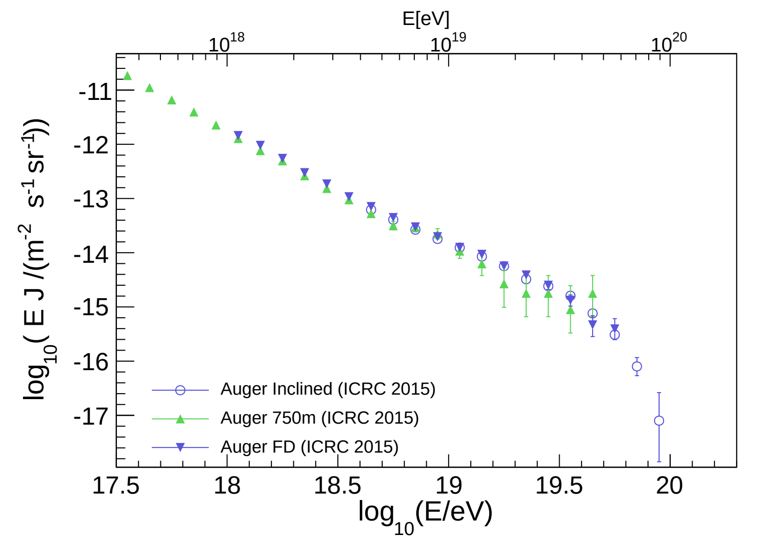

Measurements of the energy spectrum

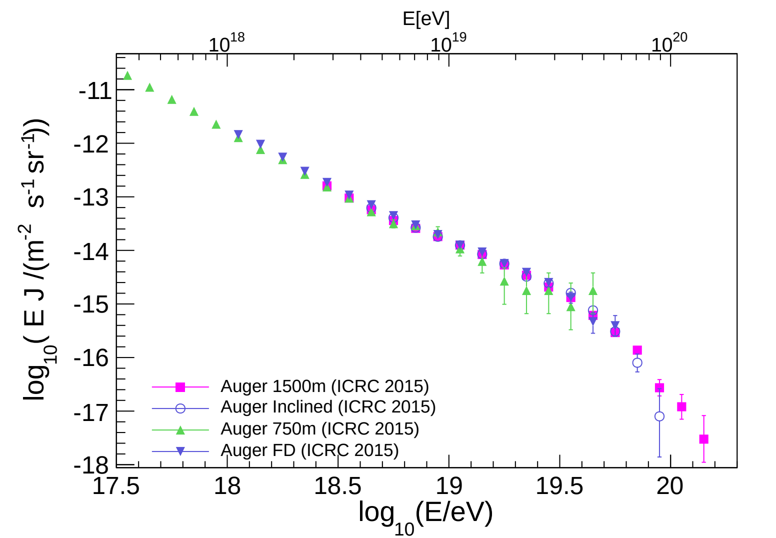

Measurements of the energy spectrum

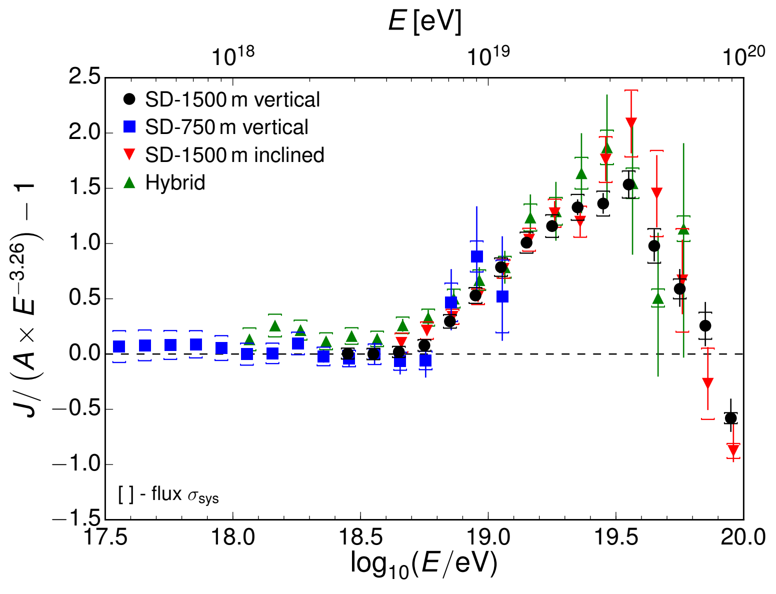

Combined energy spectrum

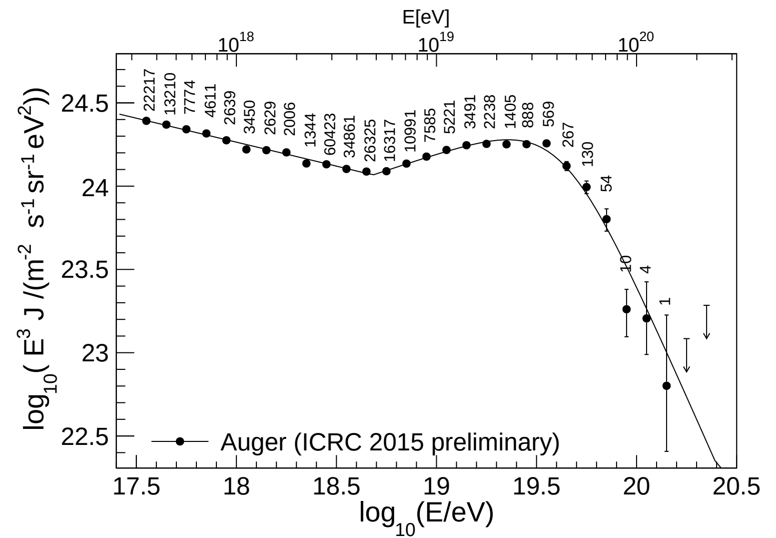

$\gamma_1 = 3.29 \pm 0.02 \pm 0.05,\ E_{tr}[eV] = 4.82 \pm 0.07 \pm 0.8$
$\gamma_2 = 2.60 \pm 0.02 \pm 0.1,\ E_s[eV] = 42.09 \pm 1.7 \pm 7.61$

Comparison with other experiments

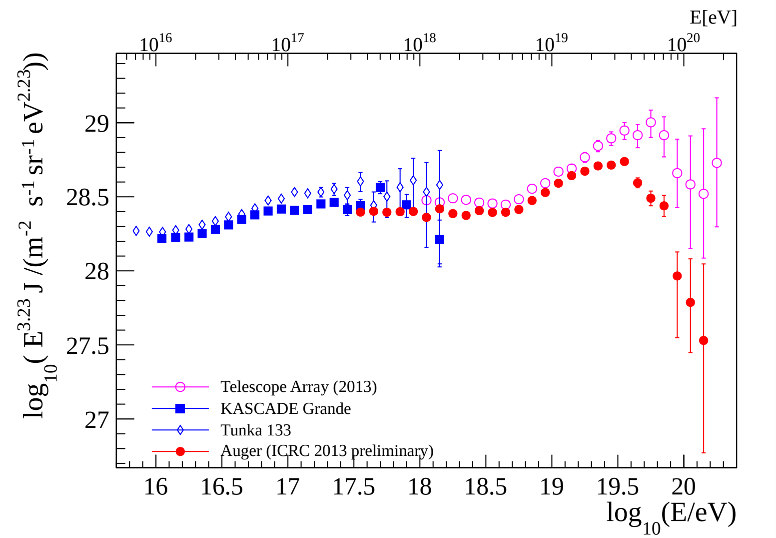

energy systematic uncertainties important

Overview of the spectral features

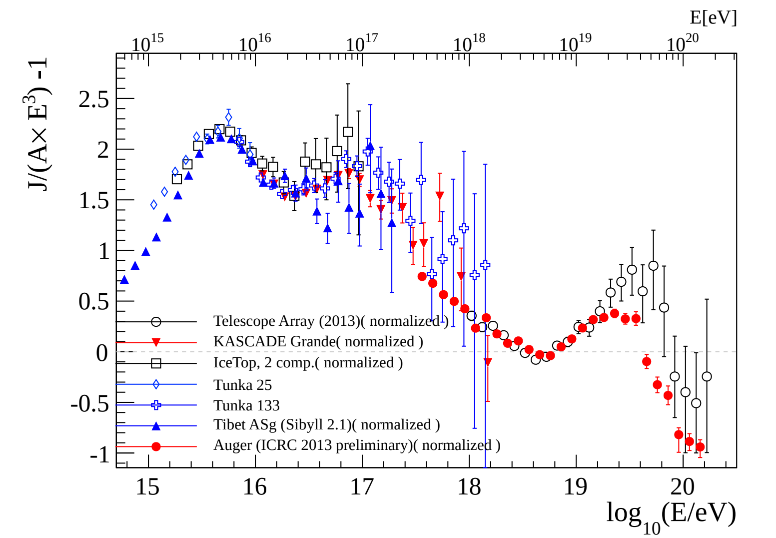

energy systematic uncertainties important

Mass composition: Cascade development

Air-showers induced by: photons or hadrons
Electromagnetic part: Heitler model
Hadronic part: Mathews-Heitler model

HeCo (HEAT+CO): extended field of view

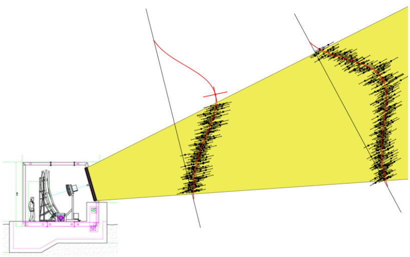

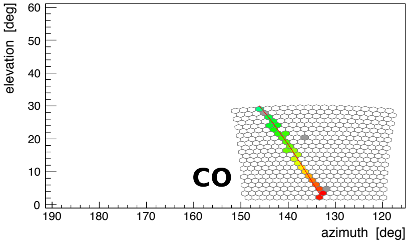

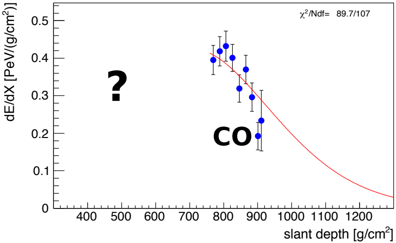

HeCo (HEAT+CO): extended field of view

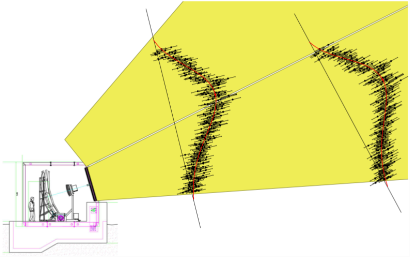

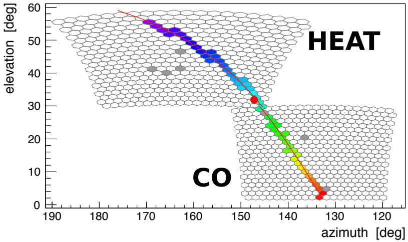

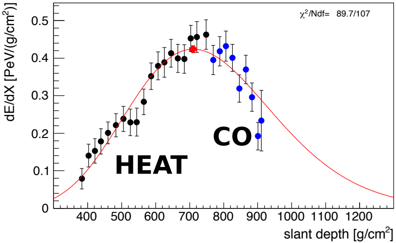

Mass composition with FD

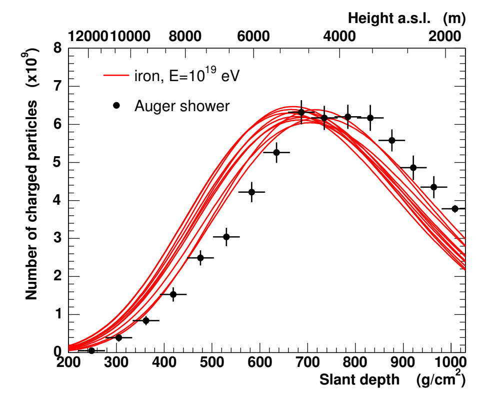

- heavier particles develop higher in the atmosphere, with less fluctuations
- $X_{\max}$ and RMS($X_{\max}$) the most sensitive parameters to chemical composition

Mass composition with FD

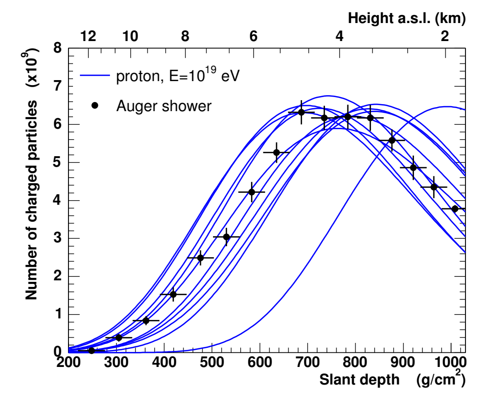

- heavier particles develop higher in the atmosphere, with less fluctuations
- $X_{\max}$ and RMS($X_{\max}$) the most sensitive parameters to chemical composition

Mass composition with FD

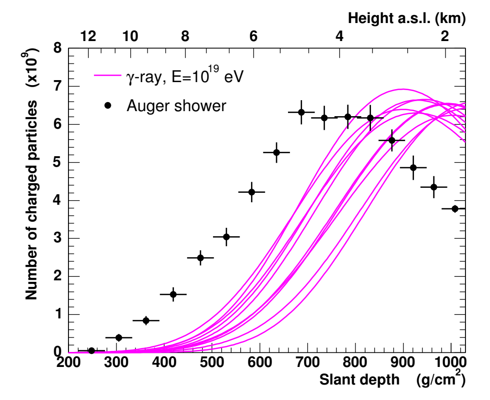

- heavier particles develop higher in the atmosphere, with less fluctuations
- $X_{\max}$ and RMS($X_{\max}$) the most sensitive parameters to chemical composition

Moments of X_{max} distributions

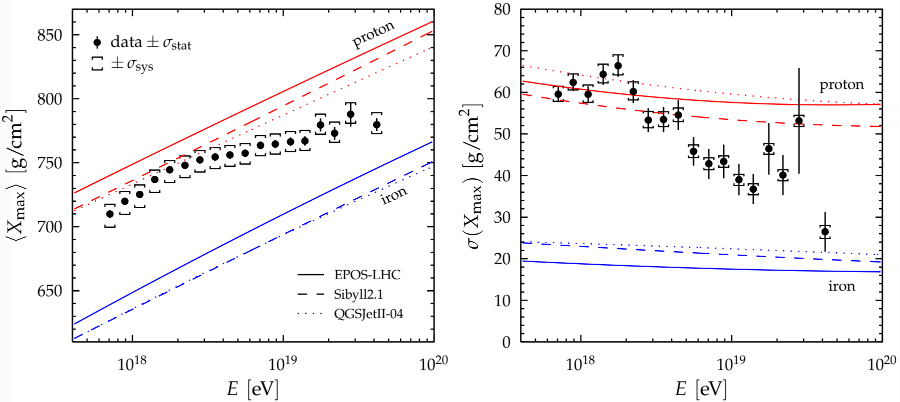

systematic uncertainties $<$10 g/cm^2 and resolution $<$ 25 g/cm^2

elongation rate changes:

$86.4 \pm 5(stat)^{+3.8}_{-3.2}(sys) g/cm^2/decade$

to

$26.4 \pm 2.5(stat)^{+7}_{-1.9}(sys) g/cm^2/decade$

Full distributions

Distributions become narrow at the highest energies

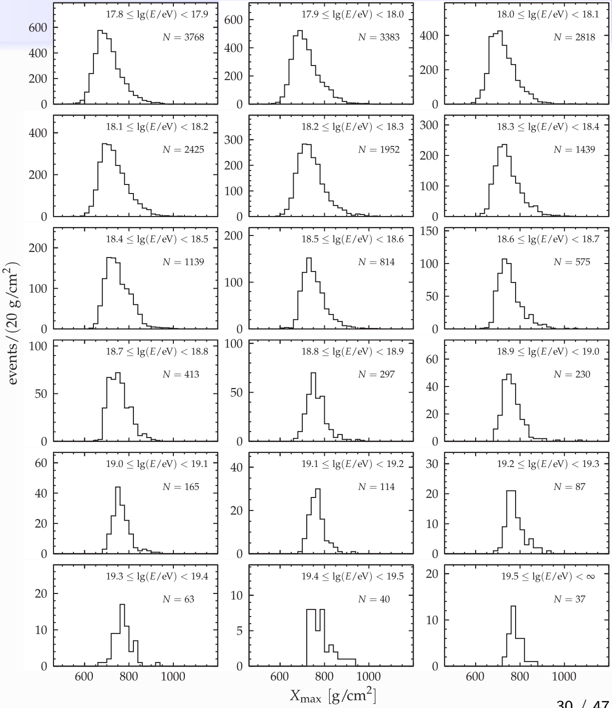

Full distributions

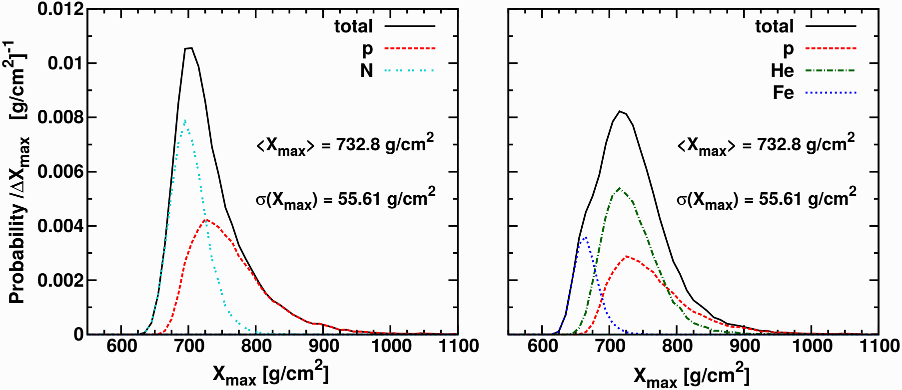

Using simulation templates and full distributions fits one can obtain the fractions of individual elements

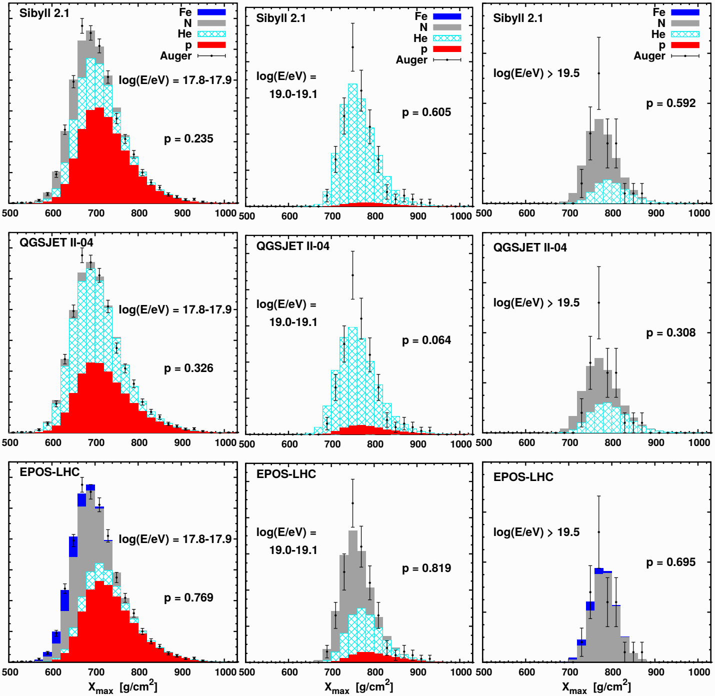
Sibyll 2.1
Fe
N
He
p
Auger
log(E/eV) = 17.8-17.9
p = 0.235
log(E/eV) =
19.0-19.1
p = 0.605
log(E/eV) > 19.5
p = 0.592
QGSJET II-04
p = 0.326
p = 0.064
p = 0.308
EPOS-LHC
p = 0.769
p = 0.819
p = 0.695
500
600
700
800
900
1000
X_{max} [g/cm^2]

Mass fractions

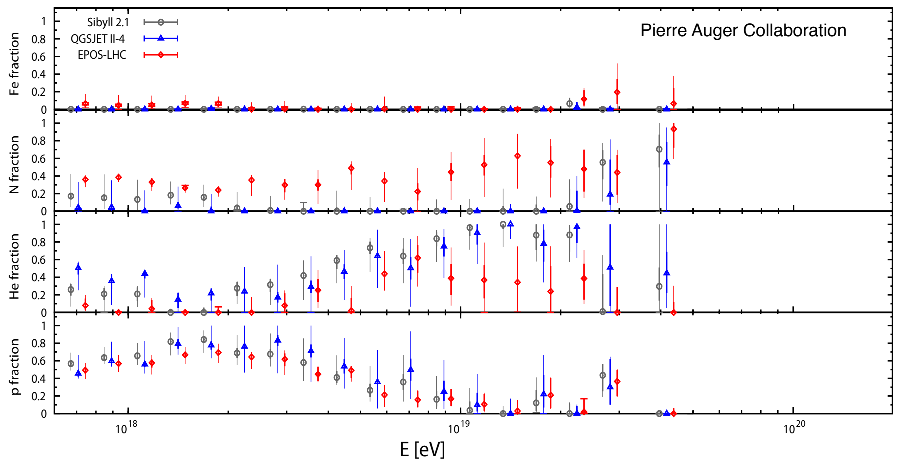

Photon limits

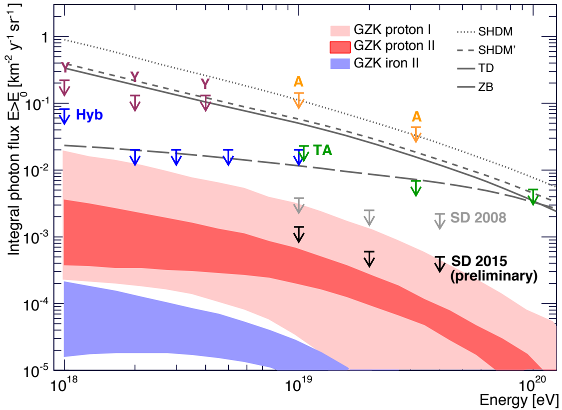

Photon searches

- steep lateral distribution function
- slow risetime of the signals
- large curvature of the shower front
- deep $X_{\max}$

Current limits exclude exotic, super-heavy relic models

Neutrino limits

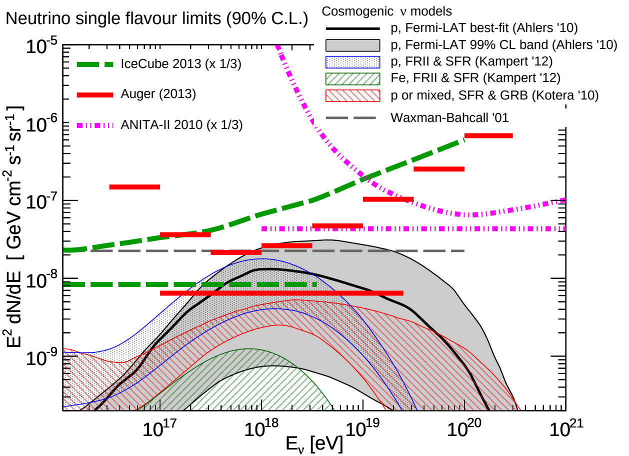

Neutrino searches

- particles that traverse the Earth (Earth-skimming)
- particles that traverse the Andes (down-going)
- interaction just above the detector
- very young air-showers

Cosmogenic neutrinos with an assumption of pure p composition at the source are disfavoured

Number of muons versus $X_{\max}$

10 EeV, 38 degrees

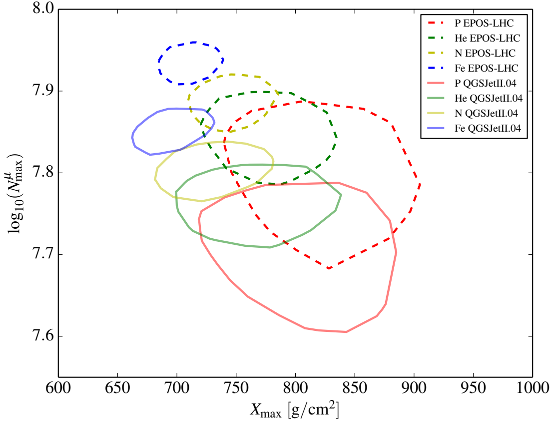

Muons may even outperform $X_{\max}$ at the highest energies!

$X_{\max}$ from SD: on ground, for a fixed energy, age, and geometry the lateral distribution functions (LDF) are universal

Key features of the upgrade

1) New electronics for the Surface Detector

$\rightarrow$ faster sampling, larger dynamic range, better triggers

2) Enhanced muon measurements with the Surface Detector

Two options (out of five) under study

a. vertical segmentation of the tanks

b. add scintillator on top of the tanks (winning project)

3) Extended operation of the Fluorescence Detector

$\rightarrow$ may double observation time

4) Array with shielded muon detectors

$\rightarrow$ energy range 1-10 EeV, O(100 km^2)

a. scintillators shielded by tank and concrete

b. scintillators shielded by 1.5 m of soil

LSD: Layered surface detector

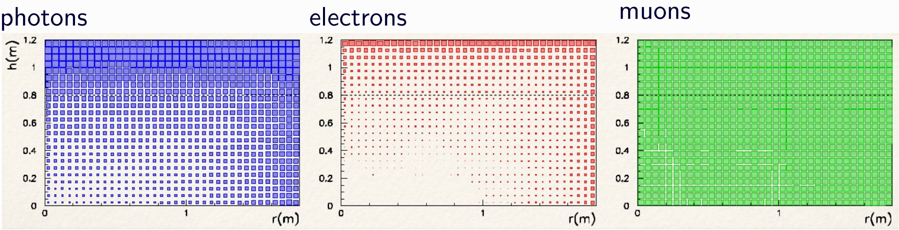

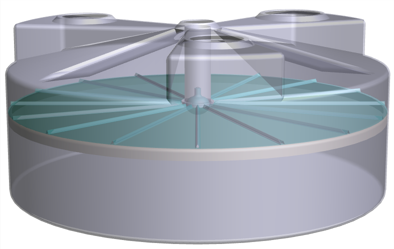

3 top PMTs
1 bottom PMT

- separation: 40/80 cm
- use known interaction characteristics of $\gamma/e^{\pm}$ and $\mu^{\pm}$
- obtain the muonic and em signal through a simple matrix inversion

(Letessier-Selvon et al., NIM A767 (2014))

LSD: Muonic and electromagnetic signals

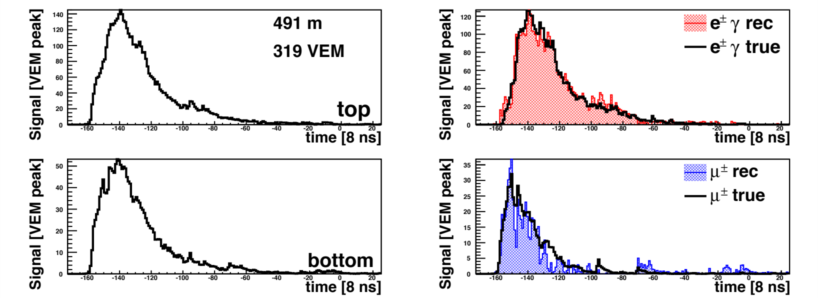

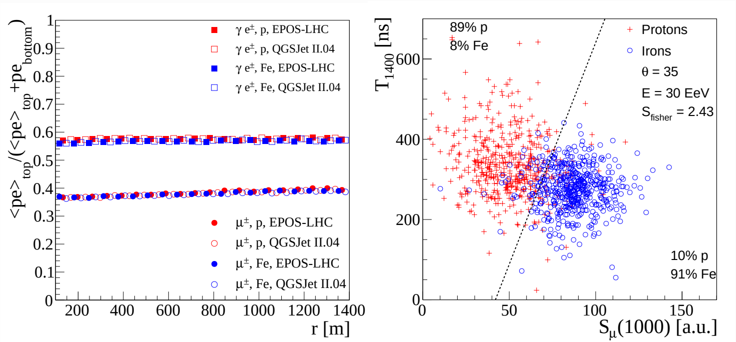

Guapa Guerrera, born on 26th of February


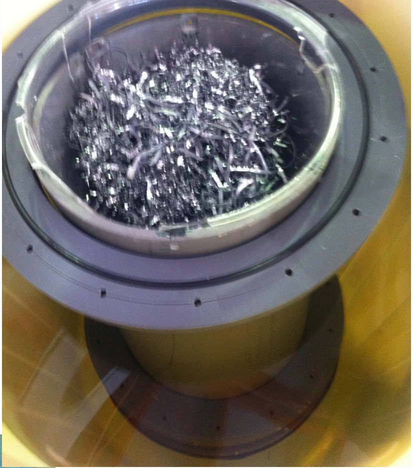
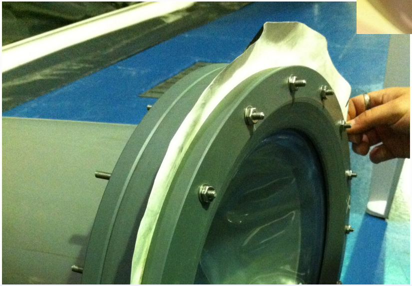
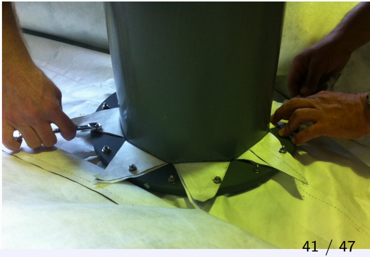

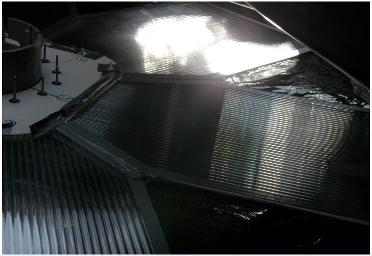

LSD prototype results

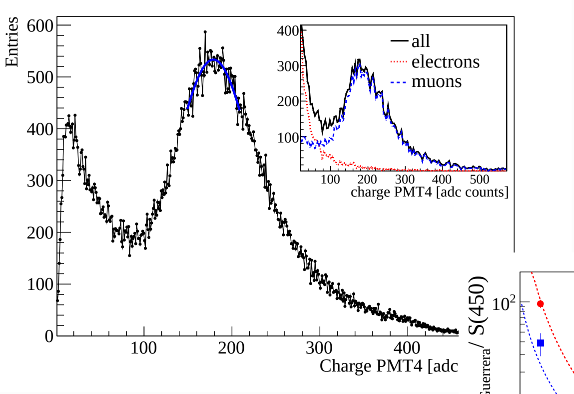

calibration with atmospheric muons

lateral distribution function

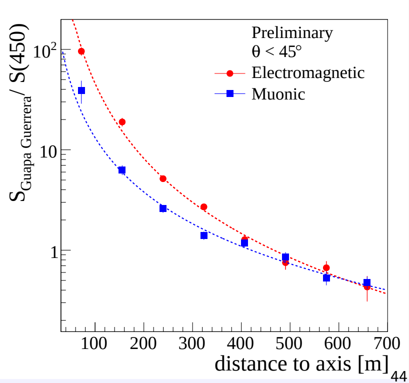

Enhanced Muon Counting: ASCII

→ 1cm thick scintillator on top of the tank

From simulations:

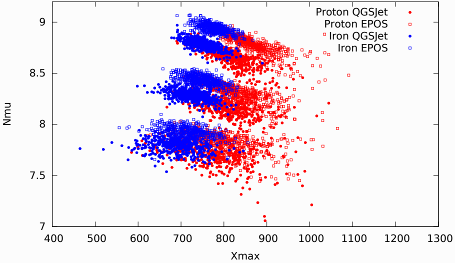

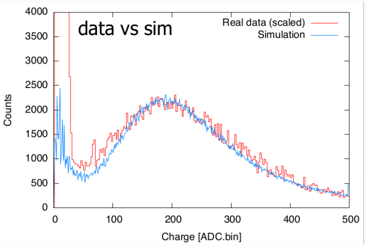

Thank you!